

Original Research

Mechanism of *Dendrobium Nobile* Polysaccharide Inhibition of Ferroptosis in Rats with Spinal Cord Injury

Jian Huang^{1,†}, Jianghong Luo^{2,†}, Ying Huang^{3,†}, Linghong Wang¹, Haibing Zhu¹, Zhengnan Li^{4,*}, Jianping Chen^{4,*}¹Department of Neurology, The First Affiliated Hospital of Gannan Medical University, 341000 Ganzhou, Jiangxi, China²School of Public Health and Health Management, Gannan Medical University, 341000 Ganzhou, Jiangxi, China³Department of Neurology, Jinshan Hospital of Fudan University, 201508 Shanghai, China⁴Department of orthopaedics, Ganzhou People's Hospital, 341000 Ganzhou, Jiangxi, China*Correspondence: 277632763@qq.com (Zhengnan Li); cjp0101@126.com (Jianping Chen)

†These authors contributed equally.

Academic Editor: Nuno A. Silva

Submitted: 25 July 2023 Revised: 17 September 2023 Accepted: 22 September 2023 Published: 21 March 2024

Abstract

Background: It has been reported that ferroptosis participates in the pathophysiological mechanism of spinal cord injury (SCI). Our preliminary experiments verified that dendrobium nobile polysaccharide (DNP) improved the behavioral function of SCI rats. Therefore, the purpose of this study was to examine the role of DNP on ferroptosis and its neuroprotective mechanism in SCI rats. **Methods:** Adult female sprague dawley (SD) rats were exposed to SCI by Allen's method, followed by an intragastric injection of 100 mg/kg DNP per day for 2 weeks. Behavioral features were verified by the Basso-Beattie-Bresnahan (BBB) scale and footprint evaluation. Iron content and glutathione (*GSH*) were assessed spectrophotometrically. Mitochondrial morphology was examined by transmission electron microscopy. The expression of ferroptosis-related genes, including System Xc⁻ light chain (*xCT*), G-rich RNA sequence binding Factor 1 (*GRSF1*) and glutathione peroxidase 4 (*Gpx4*), was examined by real-time polymerase chain reaction (PCR) and western blot. The spinal cavity was defined using hematoxylin–eosin (HE) staining, and neuronal modifications were detected by immunofluorescence. **Results:** Compared with the SCI group, the BBB score of rats in the DNP group increased at 7 d, 14 d, 21 d, and 28 d. The differences between the two groups were statistically significant. At 12 h post-injury the iron content began to decrease. At 24 h post-injury the iron content decreased significantly in the DNP group. The morphological changes of the mitochondrial crest and membrane in the DNP group were ameliorated within 24 h. Compared with the sham group, the expression of *xCT*, *GSH*, *Gpx4*, and *GRSF1* were significantly reduced after SCI. After DNP treatment, the expression of *xCT*, *Gpx4*, and *GSH* were higher. The tissue cavity area was significantly reduced and the amount of NeuN⁺ cells was increased in the DNP group at 14 d and 28 d after SCI. **Conclusions:** DNP facilitated the post-injury recovery in SCI rats via the inhibition of ferroptosis.

Keywords: spinal cord injury; dendrobium nobile polysaccharides; ferroptosis; *Gpx4*; *GRSF1*

1. Introduction

Traumatic spinal cord injury (SCI) consists of the primary injury (initial mechanical impact) and the secondary cascade of biochemical and molecular events [1]. Typically, primary mechanical injury is usually irreversible due to direct cell death, while cell death can be prevented by intervening in secondary injury [2,3]. Therefore, effectively modulating secondary injury is the key to injured spinal cord repair. However, the mechanisms underlying secondary injury are very complex, including the inflammatory response, excitatory toxic effects of glutamate, apoptosis, oxidative stress response, accumulation of neurotransmitters, lipid peroxidation, and production of reactive oxygen species (ROS) [4–6]. Recent studies have documented that ferroptosis is also implicated in the SCI secondary injury process [7,8].

Ferroptosis, a mode of programmed cell death activated by the accumulation of ROS and iron, is manifested

by cellular mitochondrial atrophy, increased bilateral membrane density, and loss of mitochondrial inner membrane cristae in morphology [9–11]. System Xc⁻ light chain (*xCT*) is a decisive regulator of ferroptosis upon diverting glutamate out of the cell in exchange for cysteine import [12]. Cysteine is a precursor for the synthesis of glutathione (*GSH*), which is a reducing agent for glutathione peroxidase 4 (*Gpx4*). *Gpx4* is an enzyme for ROS clearance and is also a representative trademark of ferroptosis [13,14]. Reduction in *GSH* synthesis inhibits the activity of *Gpx4*, which fails to neutralize intracellular lipid oxides. Afterwards, the lipid is oxidized by Fe²⁺ in a Fenton reaction, resulting in ROS accumulation and ferroptosis of cells [15]. However, the regulatory role of *Gpx4* in ferroptosis after SCI has not been fully clarified. Wang *et al.* [16] constructed a protein interaction network using the STRING database and found an obvious interaction between G-rich RNA sequence binding Factor 1 (*GRSF1*) and *Gpx4* protein.



Dendrobium nobile polysaccharide (DNP), the main component of *Dendrobium nobile*, is a traditional Chinese medicine that has antioxidative, anti-lipid peroxidation, anti-inflammatory, anti-apoptotic, and immune-modulating effects [17,18]. Herein, we discovered that DNP ameliorated the behavioral dysfunction of SCI rats. Nevertheless, the protective mechanism of DNP in SCI rats remains unclear. In this study, a modified Allen's test [19] was performed, and the Basso-Beattie-Bresnahan (BBB) score and footprint test were used to evaluate whether DNP can ameliorate the behavioral dysfunction of SCI rats. At the same time, by measuring the effect of DNP on ferroptosis in SCI rats, the potential molecular mechanism was uncovered, which laid a theoretical foundation for DNP treatment of SCI.

2. Materials and Methods

2.1 Medicine, Animals, and Treatment

Dendrobium nobile was bought from the Chinese planting base in Chishui (Guizhou, China). The polysaccharide was isolated using water extraction and alcohol precipitation, and purified to 98.1% by a DEAE Sepharose Fast Flow (57407-08-6, Bio-Resin, Beijing, China) column.

Specific pathogen Free (SPF)-grade healthy female Sprague Dawley (SD, purchased from Hunan SJA Laboratory Animal Company, Changsha, Hunan, China) rats, aged 12–14 weeks and weighing 220–250 g, were employed in our experiment. The rats were housed by the Animal Center of Gannan Medical University. Animal use and care protocols conformed to the principle of the National Institutes of Health (NIH) of China and were approved by the Ethics Committee of the first affiliated hospital of Gannan Medical University (No. GYYFY2022-10).

The experiment design is shown in Fig. 1. The experimental rats were divided into three groups: the sham operation group, the SCI group, and the DNP group. In the sham group, the lamina was simply cut off, but the spinal cord was not damaged. A modified Allen's SCI method at T10–T11 was used for the SCI and DNP groups [19]. Following injury, the DNP group was intragastrically administered 100 mg/Kg DNP (purity 98%, Chengdu Alfa Biotechnology Co., Ltd., Chengdu, China) once a day for 14 consecutive days, and the other two groups were intragastrically administered equal amounts of normal saline.

2.2 BBB Score and Footprint Analysis

The BBB scale, to observe the walking, trunk movement, and coordination of the hip, knee, and ankle joints by rats crawling, and footprint analysis were used to rate the recovery of hind limb motor function, scoring from 0 to 21. Hind limb motor function was valued at 1, 3, 7, 14, 21, and 28 days after SCI.

In the footprint analysis test, rats' hind paws were stained with red ink, and their forepaws were stained with black ink. The rats then walked through a narrow tunnel of

60 cm in length and 7.5 cm wide. The opposite end of the tunnel was illuminated to guide the movement of the rats. The bottom of the tunnel was covered with white test paper. The evaluation indicator was clarity of footprint.

2.3 Determination of Iron and GSH Content

The injured segmental spinal cord was sampled at 12, 24 and 48 hours after SCI. Spinal cord tissue was homogenized mechanically to obtain supernatant under ice water bath conditions. Iron content was detected using a tissue iron determination kit (A039-2-1; Nanjing Jiancheng, Nanjing, Jiangsu, China), according to the manufacturer's instructions, and GSH content was determined using a glutathione assay kit (A006-2-1, Nanjing Jiancheng), with the bicinchoninic acid (BCA) method, according to the manufacturer's instructions.

2.4 Transmission Electron Microscopy

At 24 h after SCI, the injured spinal cord tissue was quickly removed and made into 1 mm × 1 mm × 1 mm blocks. Tissue was fixed with 2.5% glutaraldehyde in a 0.1 M phosphate buffer (pH 7.4) for 2 h at room temperature, and then treated with 1% samarium tetroxide at 0.1 M phosphate buffer (PB) [20]. Photographs were then taken using transmission electron microscopy (TEM) (7600TEM, Hitachi, Tokyo, Japan).

2.5 Western Blot

Spinal cord tissue was dissolved in radio-immunoprecipitation assay (RIPA) lysis buffer. The protein level was measured using a bicinchoninic acid assay (BCA) protein analysis kit (Beyotime, Shanghai, China). Fifty micrograms of protein were separated on a 10% or 12% sodium dodecyl sulfate polyacrylamide gel and transferred to a polyvinylidene fluoride (PVDF) membrane. After being incubated with 5% albumin from bovine serum (BSA) for 1 h, the membrane was incubated overnight on a shaker with primary antibody. The primary antibodies included rabbit anti-*xCT* (diluted at 1:1000, Boster, Wuhan, Hubei, China), mouse anti-*Gpx4* (diluted at 1:2000, Proteintech, Shanghai, China), rabbit anti-*GRSFI* (diluted at 1:1000, Abcam, Boston, MA, USA), and mouse anti-GAPDH (diluted at 1:1000, Beyotime, Wuhan, Hubei, China). After washing with tris buffered saline + tween (TBST) three times, the secondary antibody (A0216, Beyotime, Shanghai, China) was coupled with a 1:10,000 dilution of horseradish peroxidase and incubated at room temperature for 1 h. Finally, a Chemi Dox XRS chemiluminescence imaging system (Bio-Rad, San Francisco, CA, USA) was used to visualize the signal. All tests were replicated three times.

2.6 Real-Time PCR

Spinal cord tissue specimens were removed from the freezer at –80 °C. cDNA (2 μL) was quantified accord-

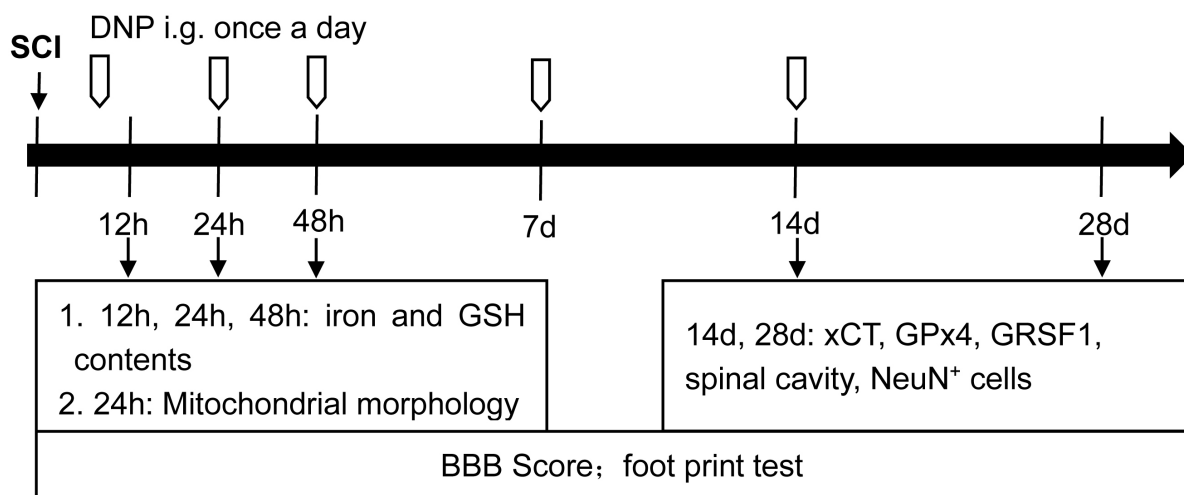


Fig. 1. Schematic design of the experiment. SCI, spinal cord injury; DNP, dendrobium nobile polysaccharide; *GSH*, glutathione; *Gpx4*, glutathione peroxidase 4; *GRSF1*, G-rich RNA sequence binding factor 1; BBB, Basso-Beattie-Bresnahan; *xCT*, Xc^- light chain; i. g., oral gavage.

Table 1. Primer information

Gene	Primer sequences
<i>xCT</i>	
Forward primer	5'-GCT GTT ATT GTT TTG CAT CCT CT -3'
Reverse primer	5'-TCT GGG CGT TTG TAT CGA AG -3'
<i>Gpx4</i>	
Forward primer	5'-CCG TCT GAG CCG CTT ATT -3'
Reverse primer	5'-CAC GCA ACC CCT GTA CTT AT -3'
<i>GRSF1</i>	
Forward primer	5'-TAC TGC CAG GAG TCC AAA AC-3'
Reverse primer	5'-ACA TAC CGC TGC CCC AT -3'
β -actin	
Forward primer	5'-GCC ATG TAC GTA GCC ATC CA -3'
Reverse primer	5'-GAA CCG CTC ATT GCC GAT AG -3'

ing to the manufacturer's instructions. Data are shown using $2^{-\Delta\Delta C_t}$ values [21]. Primer design, synthesis, and sequences of target genes were derived from the database (<https://www.ncbi.nlm.nih.gov/gene/?term=>), and carried out by GENERAL Biosystems (Anhui) Corporation Limited (Chuzhou, Anhui, China) (Table 1).

2.7 Hematoxylin–Eosin Staining

Rats were sacrificed by intraperitoneal injection of 10% sodium pentobarbital (3.5 mL/kg, 57-33-0, Damao chemical reagent factory of Tianjin, Tianjin, China). The heart was then infused with saline and 4% formaldehyde. After perfusion, the injured central spinal cord segment (0.5 cm long) was taken and immediately stored in 4% formaldehyde. The spinal cord, soaked in formaldehyde, was dehydrated and embedded; it was then sectioned horizontally into 4 μ m slices [22]. For immunofluorescence experiments, the preparation process of tissue specimens was the

same as described above. The tissue was then stained according to the hematoxylin–eosin (HE) staining kit instructions (Solarbio, Beijing, China).

2.8 Immunofluorescence

Paraffin sections of spinal cord specimens were prepared and 0.1% BSA was added to cover the specimens completely. The slices were placed in a wet box at room temperature for 15 minutes. The primary antibody (NeuN, Proteintech, 1:100) was diluted with phosphate buffered saline (PBS) solution, dropped onto the slices, and then placed in a refrigerator at 4 °C overnight. The slices were removed and washed with PBS. The secondary antibody was dropped onto the sections of the spinal cord specimen, and the slices were left standing at room temperature for 1 hour (in the dark), and then were removed and washed with PBS. Drops of 4',6-Diamidino-2-Phenylindole (DAPI) were added until the specimen was completely covered.

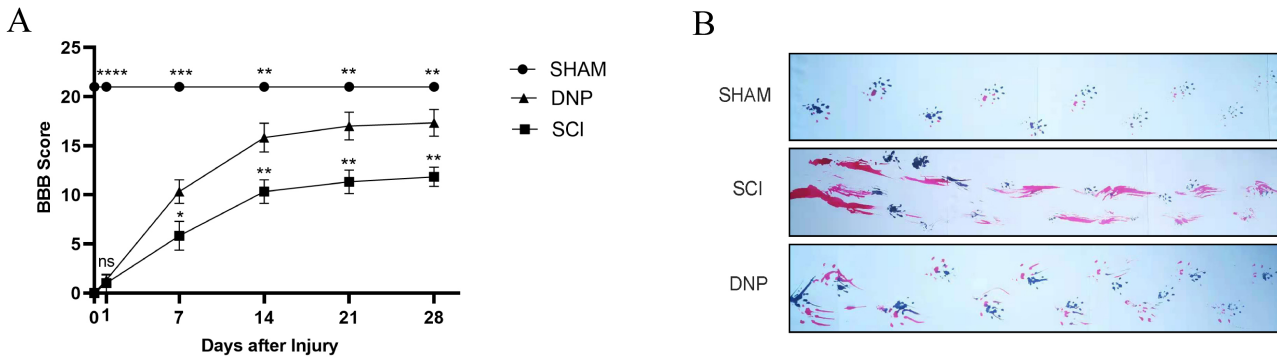


Fig. 2. The effect of DNP on hind limb function of SCI rats. (A) BBB scores of different groups at 1, 7, 14, 21, 28 d post-SCI (values are expressed as the mean \pm SE. $n = 3$, $^{ns}p > 0.05$, $^{*}p < 0.05$, $^{**}p < 0.01$, $^{***}p < 0.001$, $^{****}p < 0.0001$ vs the DNP group). (B) Footprint of three groups at 28 d post-injury. SE, standard error; ns, not significant.

Finally, drops of anti-fluorescence quenching agent were added and the specimen was sealed with cover glass. Photos were captured under a fluorescence microscope (DM2500, Leica, Berlin, Germany).

2.9 Statistical Analysis

Statistical analyses were carried out using SPSS 20.0 statistical software (SPSS Inc., Chicago, IL, USA). Data are represented as the mean \pm standard error (SE). Repeated measures analysis of variance (ANOVA) was performed for comparisons between two groups and multiple groups. $p < 0.05$ was deemed statistically significant.

3. Results

3.1 DNP Promotes the Hind Limb Function in SCI Rats

The rats were evaluated at 1, 7, 14, 21, and 28 days post-injury. On day 1, the mean BBB scores of the sham group were 21 points, those of the SCI group were 1 point, and those of the DNP group were 1.5 points, but the differences were not statistically significant between the SCI and the DNP groups ($p > 0.05$). At 7, 14, 21, and 28 days, the scores of the DNP group were markedly increased compared with the SCI group ($p < 0.05$). Although the BBB scores were increased as time progressed, the scores in the DNP and SCI groups were decreased compared with the sham group ($p < 0.05$) (Fig. 2A).

The footprint test showed that rats in the sham group had clear footprints and no drag on the hind limbs. In the SCI group, the drag of the hind limbs was obvious, and footprints were not distinguishable. The footprints in the DNP group were clearer than those in the SCI group, but there were still drag marks (Fig. 2B).

3.2 DNP Decreases Iron Content and Facilitates Mitochondrial Morphology in the Injured Spinal Cord

Iron content was increased significantly after SCI, but gradually decreased over time. After DNP treatment, the iron content decreased at 12 h post-injury, but there were

no marked differences compared with the SCI group ($p > 0.05$). However, the iron content decreased significantly compared with the SCI group at 24 h and 48 h post-injury ($p < 0.05$) (Fig. 3A).

We observed ultrastructural changes in mitochondria in injured spinal cord using TEM within 24 h after SCI. The mitochondrial crest and membrane were intact in the sham group. In the SCI group, the mitochondrial membrane was disrupted and the crest almost vanished. Compared with the SCI group, the mitochondrial crest and membrane in the DNP group were improved (Fig. 3B).

3.3 DNP Increases the mRNA and Protein Levels of GSH, xCT, Gpx4, and GRSF1

We measured the mRNA and protein expression of xCT, Gpx4, GRSF1, and GSH after SCI. Compared with the sham group, the xCT, Gpx4, and GSH levels in the SCI group were markedly reduced at 14 d and 28 d after SCI ($p < 0.05$). After DNP treatment, the mRNA and protein expression of xCT, Gpx4, and GSH were upregulated, suggesting that DNP could prevent ferroptosis by upregulating the expression of GSH, xCT, and Gpx4. In addition, the level of mRNA and protein expression of xCT and Gpx4 in the DNP group at 28 d were significantly increased compared with that at 14 d ($p < 0.05$), suggesting that the inhibition of ferroptosis in SCI by DNP continued with the DNP treatment duration (Figs. 4,5). Meanwhile, the mRNA and protein level trends of GRSF1 and Gpx4 were the same compared with each other. Since GRSF1 and Gpx4 interact with each other and GRSF1 is the upstream protein of Gpx4, we believed that DNP increased the expression of Gpx4 by regulating GRSF1.

3.4 DNP Improves Injured Spinal Cord Cavities

Compared with the sham group, the damaged spinal cord transverse sections showed obvious destructive cavities. The mean value of cavity area was $5.998 \mu\text{m}^2$ at 14 days and $5.448 \mu\text{m}^2$ at 28 days in the SCI group, and 4.997

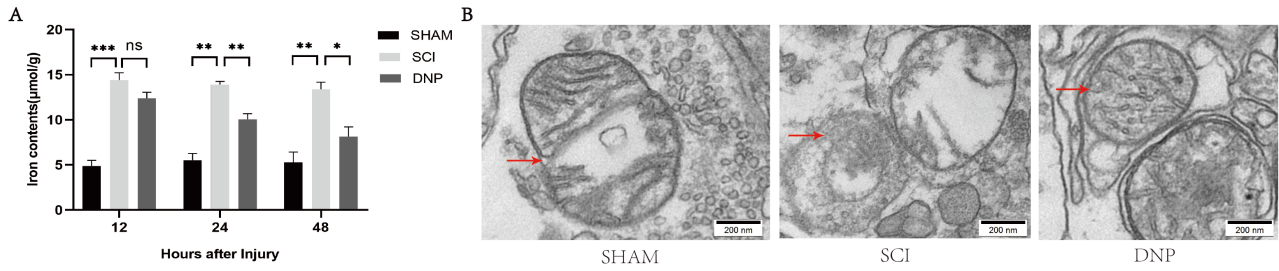


Fig. 3. Effects of DNP on iron content and mitochondrial morphology in injured spinal cord. (A) Iron content at 12, 24 and 48 hours after SCI (values are expressed as the mean \pm SE, $n = 3$. $^{ns}p > 0.05$, $^{*}p < 0.05$, $^{**}p < 0.01$, $^{***}p < 0.001$ vs the SCI group). (B) Mitochondrial form in the spinal cord tissue at 24 h after SCI (Scale bar = 200 nm). red arrow means: Outstanding performance.

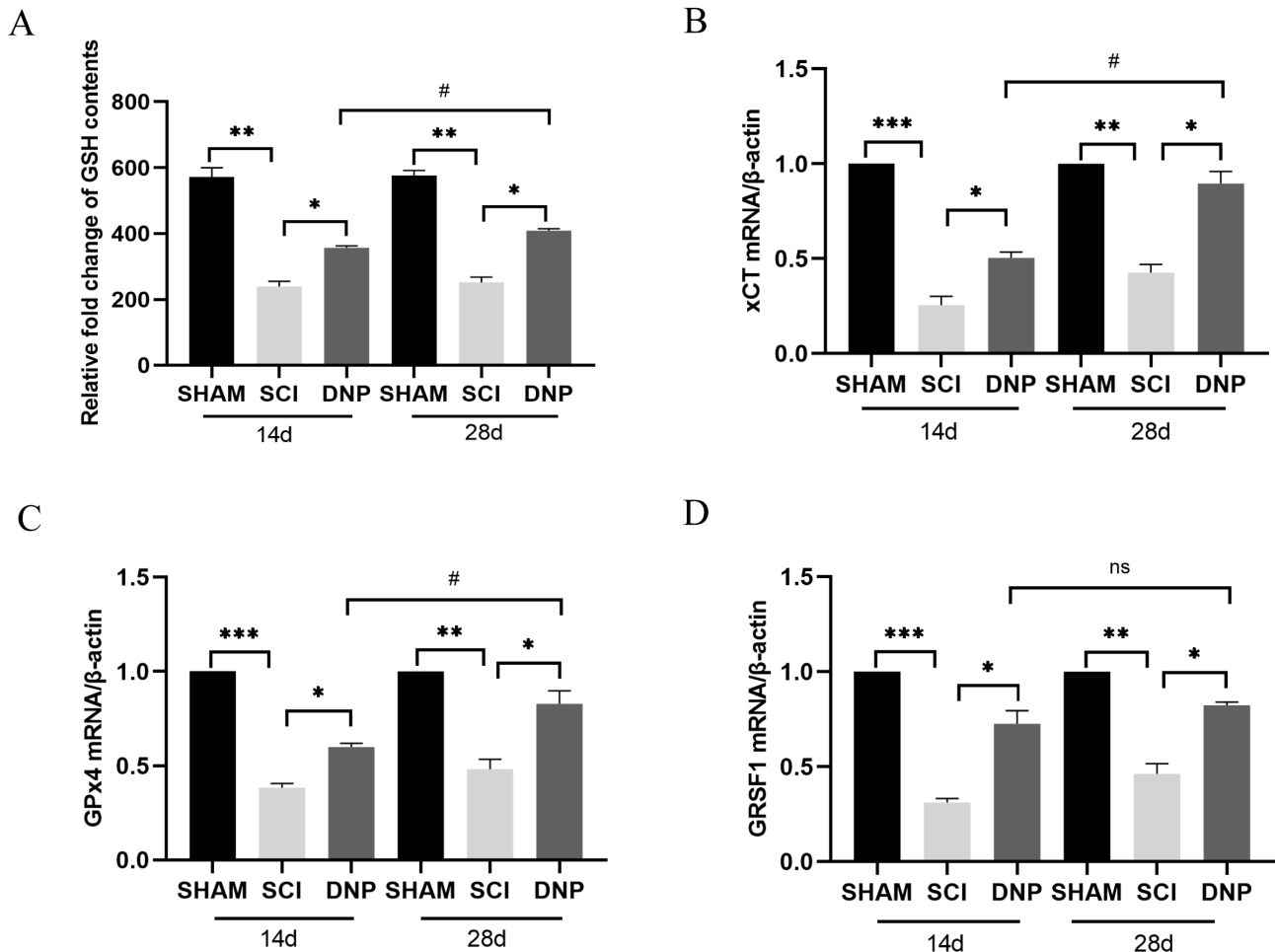


Fig. 4. Effects of DNP on GSH content and level of *xCT* mRNA, *Gpx4* mRNA, and *GRSF1* mRNA at 14 d and 28 d after SCI. (A–D) Effect of DNP on GSH content (A), *xCT* mRNA (B), *Gpx4* mRNA (C), and *GRSF1* mRNA (D) in injured spinal cord (values are expressed as the mean \pm SE, $n = 3$. $^{*}p < 0.05$, $^{**}p < 0.01$, $^{***}p < 0.001$ vs the SCI group. $^{ns}p > 0.05$, $^{#}p < 0.05$ vs the DNP group).

μm^2 at 14 days and $4.180 \mu\text{m}^2$ at 28 days in the DNP group. Compared with the SCI group, the mean tissue cavity area was markedly improved in the DNP group (14 d SCI vs 14 d DNP: $p = 0.0257$; 28 d SCI vs 28 d DNP: $p = 0.0060$). At 28 days, the cavities of the spinal cord tissue in the DNP group were smaller than at 14 days ($p = 0.0086$), and the tissue damage was relatively mild. These results suggest that

DNP treatment can repair injured spinal cord tissue, and the injured spinal cord tissue recovered to a greater extent with the prolongation of DNP treatment duration (Fig. 6).

3.5 DNP Increases the Amount of NeuN⁺ Cells after SCI

Neurons are the most vital cells in the central nervous system, and NeuN is a specific marker of neurons.

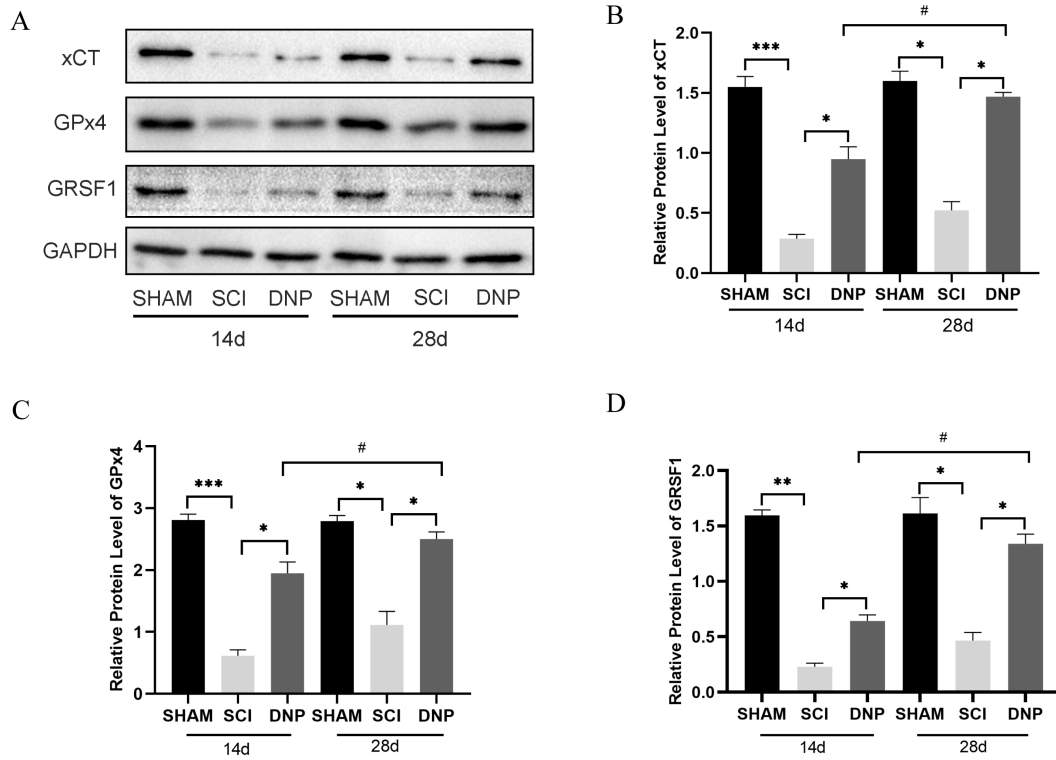


Fig. 5. Effects of DNP on *xCT*, *Gpx4*, and *GRSF1* protein level at 14 and 28 days after SCI. (A) Levels of *xCT*, *Gpx4*, and *GRSF1* at 14 and 28 days after SCI by western blot. (B–D) Levels of *xCT*, *Gpx4*, and *GRSF1* proteins were quantitatively detected (values are expressed as the mean \pm SE, $n = 3$). * $p < 0.05$, ** $p < 0.01$, *** $p < 0.001$ vs the SCI group. # $p < 0.05$ vs the DNP group).

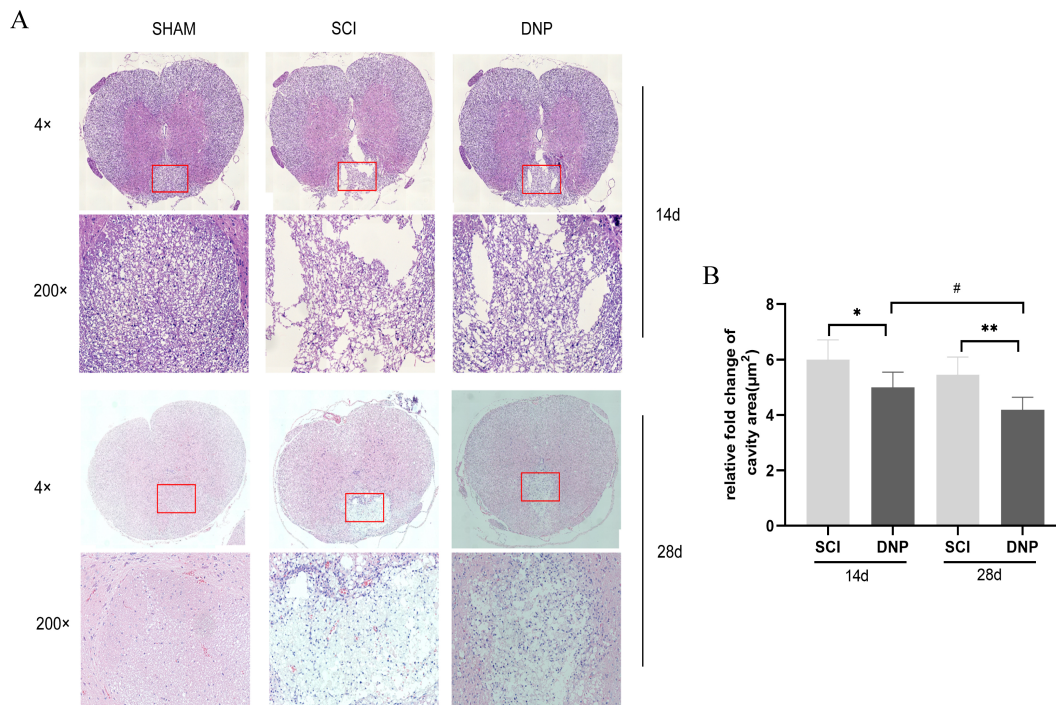


Fig. 6. Effect of DNP on histopathological changes of injured spinal cord. (A) HE staining images of the sham, SCI, and DNP groups at 14 d and 28 d of SCI (image magnification: 4 \times , 200 \times). (B) Quantification of the cavity areas (values are displayed as the mean \pm SE, $n = 3$). * $p < 0.05$, ** $p < 0.01$ vs the SCI group. # $p < 0.05$ vs the DNP group). HE, hematoxylin–eosin.

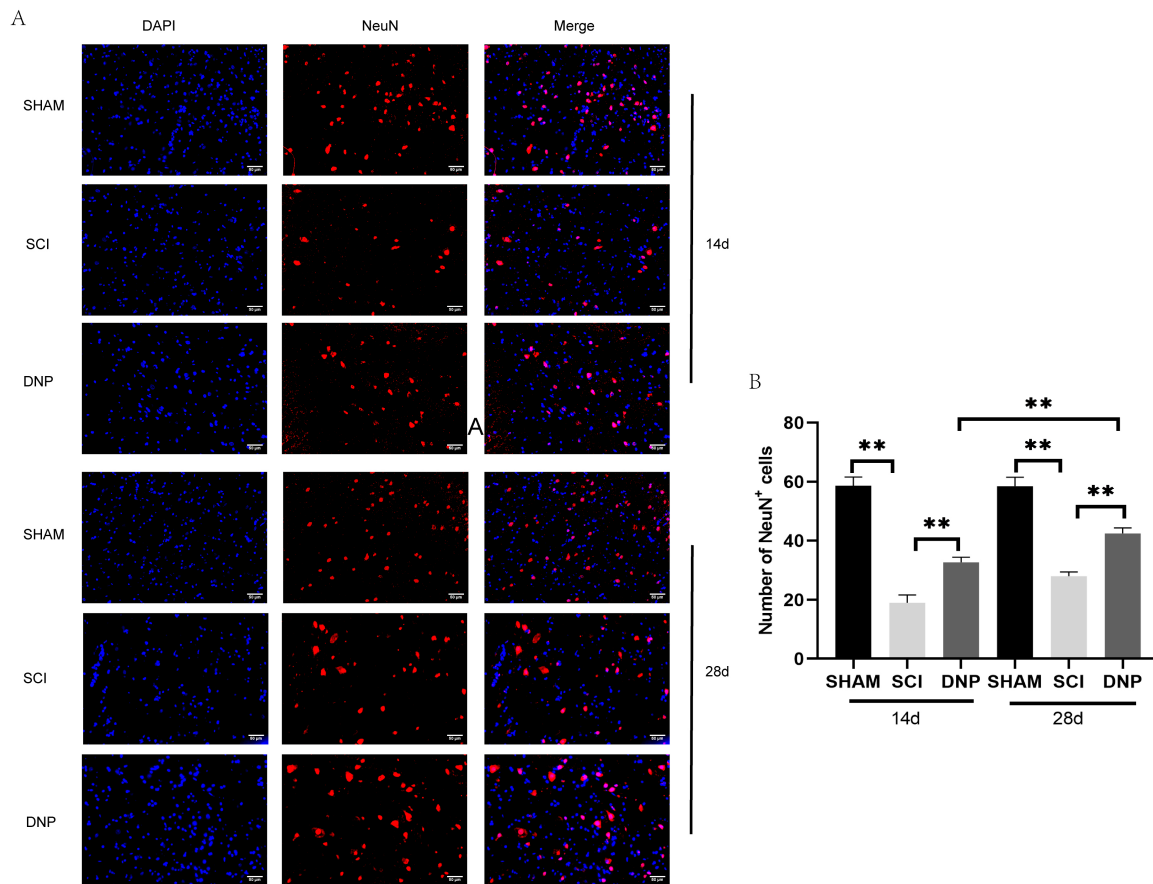


Fig. 7. Effects of DNP on the number of NeuN⁺ cells in injured spinal cord. (A) NeuN immunofluorescence staining of the injured area at 14 and 28 days after SCI, Scale bar = 50 μm. (B) Number of NeuN⁺ cells (values are displayed as the mean ± SE, n = 3. ***p* < 0.01).

The amount of NeuN⁺ positive cells was assessed by immunofluorescence assay. Compared with the sham group, the number of NeuN⁺ cells was markedly reduced in the SCI group, and DNP treatment increased the amount of NeuN⁺ cells at 14 and 28 days after SCI. Furthermore, the number of NeuN⁺ cells at 28 d was significantly greater than that at 14 d in the DNP group (*p* < 0.05). These results demonstrated that the therapeutic effect of DNP continued with the treatment duration of DNP (Fig. 7).

4. Discussion

SCI is a serious disorder affecting humans. After SCI, continuous oxidative stress, bleeding, glutamic toxicity, and other stimuli lead to serious injury [23–25]. In recent decades, researchers have sought different types of treatments for SCI, including the use of hormones, early surgery, stem cell therapy, and other drugs or means [26]. However, the outcomes have not been particularly satisfactory. The present study focused on DNP, a traditional Chinese medicine that has beneficial effects on antioxidative stress, inflammation, and lipid peroxidation. Our research found that DNP improves lower limb motor function in SCI rats. HE staining confirmed that DNP promotes spinal cav-

ity repair. Immunofluorescence assays also supported that DNP improves the recovery of neurons in injured spinal cord tissue. Collectively, these outcomes point to a neuroprotective effect of DNP.

The secondary injury process after SCI includes a series of biochemical and cellular events, such as mass neuronal death, axonal rupture, and disruption of nerve conduction pathways [27,28]. Inhibition or reduction of neuronal death is the main strategy to promote SCI recovery. To date, the manners of cell death found in SCI include apoptosis, necroptosis, pyroptosis, autophagy, and ferroptosis [5,11,29–31]. Ferroptosis, a newly discovered mechanism of cell death, has been confirmed to perform a vital role in the pathophysiological process of SCI [7,8]. Our study found that mitochondrial morphology changed, iron content was reduced, and *GSH*, *Gpx4*, and *xCT* expression decreased, confirming the existence of ferroptosis in SCI, which is consistent with a previous study by Zhang *et al.* [7]. This study further showed that DNP could reduce iron content and increase the level of *xCT*, *GSH*, and *Gpx4*, which are important biomarkers of ferroptosis. TEM revealed that the disruption of the mitochondrial crest and membrane in spinal cord tissue was

improved. These results revealed that DNP has a neuroprotective impact on SCI through preventing ferroptosis. We further explored the reduced expression of *GRSF1* and *Gpx4* in SCI. *GRSF1*, an RNA-binding protein in the nucleus and cytoplasm, was found to interact with *Gpx4*. It has been demonstrated that *GRSF1* binds to an A(G)4A membrane sequence in the 5'-untranslated region of mitochondrial *Gpx4* (m-*Gpx4*) mRNA, upregulates the expression of m-*Gpx4* mRNA at the translational level, and immune precipitates with *Gpx4*, resulting in the upregulation of *Gpx4* expression [32]. Therefore, we hypothesize that DNP resists ferroptosis in SCI by upregulating *GRSF1*, increasing the level of *Gpx4* and preventing lipid peroxidation.

Although our study confirmed that DNP has a neuroprotective role in SCI by inhibiting ferroptosis, ferroptosis pathways, such as fatty acid metabolism, (seleno)thiol metabolism, and the mevalonate pathway [33], might also be involved; these areas need to be investigated in future research. However, we sought to further clarify the mechanism by which *GRSF1* adjusts *Gpx4* expression in an *in vitro* cell model of SCI in our next study. There is some disagreement in the literature as to which rodent age equates to adulthood. We chose the 12–14-week-old female SD rat, as this is considered a relatively young adulthood SCI model according to Agoston *et al.* [34].

5. Conclusion

We demonstrated that DNP ameliorates behavioral impairment and neuronal damage, likely via the inhibition of ferroptosis, as demonstrated by the attenuated decreased *GSH*, *xCT*, *Gpx4*, and iron content in rat spinal cord. Our results shed new light on SCI and indicate that DNP is a promising neuroprotective agent.

Availability of Data and Materials

The raw data supporting the conclusions of this article will be made available by the authors. Requests to access the datasets should be directed to Ying Huang (huangying0202@126.com).

Author Contributions

ZL and YH designed the research study. JH, JC, HZ and LW conducted experiments. JL analyzed the data. All authors contributed to editorial changes in the manuscript. All authors read and approved the final manuscript. All authors have participated sufficiently in the work and agreed to be accountable for all aspects of the work.

Ethics Approval and Consent to Participate

Animal use and care protocols were in conformity to the principle of the National Institutes of Health (NIH) of China and approved by the Ethics Committee of the first affiliated hospital of Gannan Medical University (No. GYYFY2022-10).

Acknowledgment

We thank all the peer reviewers for their opinions and suggestions.

Funding

The study was supported by the Science and Technology Project of Jiangxi Provincial Education Department (No. GJJ211502, GJJ211524), the Science Project of Jiangxi Provincial Administration of Traditional Chinese Medicine (No. 2021A365 and 2022B964), the Key Laboratory of Translational Medicine of cerebrovascular disease of Ganzhou (No. 2022DSYS9855), the Science and Technology Plan Project of Ganzhou (No. GZ2023ZSF101, GZ2023ZSF107, and GZ2023ZSF363).

Conflict of Interest

The authors declare no conflict of interest.

References

- [1] Alizadeh A, Dyck SM, Karimi-Abdolrezaee S. Traumatic Spinal Cord Injury: An Overview of Pathophysiology, Models and Acute Injury Mechanisms. *Frontiers in Neurology*. 2019; 10: 282.
- [2] Ropper AE, Ropper AH. Acute Spinal Cord Compression. *The New England Journal of Medicine*. 2017; 376: 1358–1369.
- [3] Xue H, Zhang XY, Liu JM, Song Y, Liu TT, Chen D. NDGA reduces secondary damage after spinal cord injury in rats via anti-inflammatory effects. *Brain Research*. 2013; 1516: 83–92.
- [4] Duan HQ, Wu QL, Yao X, Fan BY, Shi HY, Zhao CX, *et al.* Nafamostat mesilate attenuates inflammation and apoptosis and promotes locomotor recovery after spinal cord injury. *CNS Neuroscience & Therapeutics*. 2018; 24: 429–438.
- [5] Liu M, Wu W, Li H, Li S, Huang LT, Yang YQ, *et al.* Necroptosis, a novel type of programmed cell death, contributes to early neural cells damage after spinal cord injury in adult mice. *The Journal of Spinal Cord Medicine*. 2015; 38: 745–753.
- [6] Anjum A, Yazid MD, Fauzi Daud M, Idris J, Ng AMH, Selvi Naicker A, *et al.* Spinal Cord Injury: Pathophysiology, Multimolecular Interactions, and Underlying Recovery Mechanisms. *International Journal of Molecular Sciences*. 2020; 21: 7533.
- [7] Zhang Y, Sun C, Zhao C, Hao J, Zhang Y, Fan B, *et al.* Ferroptosis inhibitor SRS 16-86 attenuates ferroptosis and promotes functional recovery in contusion spinal cord injury. *Brain Research*. 2019; 1706: 48–57.
- [8] Yao X, Zhang Y, Hao J, Duan HQ, Zhao CX, Sun C, *et al.* Deferoxamine promotes recovery of traumatic spinal cord injury by inhibiting ferroptosis. *Neural Regeneration Research*. 2019; 14: 532–541.
- [9] Xie Y, Hou W, Song X, Yu Y, Huang J, Sun X, *et al.* Ferroptosis: process and function. *Cell Death and Differentiation*. 2016; 23: 369–379.
- [10] Fang S, Yu X, Ding H, Han J, Feng J. Effects of intracellular iron overload on cell death and identification of potent cell death inhibitors. *Biochemical and Biophysical Research Communications*. 2018; 503: 297–303.
- [11] Zeng H, You C, Zhao L, Wang J, Ye X, Yang T, *et al.* Ferroptosis-Associated Classifier and Indicator for Prognostic Prediction in Cutaneous Melanoma. *Journal of Oncology*. 2021; 2021: 3658196.
- [12] Yu H, Guo P, Xie X, Wang Y, Chen G. Ferroptosis, a new form of

- cell death, and its relationships with tumourous diseases. *Journal of Cellular and Molecular Medicine*. 2017; 21: 648–657.
- [13] Conrad M, Friedmann Angeli JP. Glutathione peroxidase 4 (*Gpx4*) and ferroptosis: what's so special about it? *Molecular & Cellular Oncology*. 2015; 2: e995047.
- [14] Imai H, Matsuoka M, Kumagai T, Sakamoto T, Koumura T. Lipid Peroxidation-Dependent Cell Death Regulated by *Gpx4* and Ferroptosis. *Current Topics in Microbiology and Immunology*. 2017; 403: 143–170.
- [15] Latunde-Dada GO. Ferroptosis: Role of lipid peroxidation, iron and ferritinophagy. *Biochimica et Biophysica Acta. General Subjects*. 2017; 1861: 1893–1900.
- [16] Wang S, Wang B, Chen J. Clinical significance of expression of *Gpx4* in gastric cancer. *Chinese Journal of Clinicians (Electronic Edition)*. 2019; 13: 498–503. (In Chinese)
- [17] Wang D, Fan B, Wang Y, Zhang L, Wang F. Optimum Extraction, Characterization, and Antioxidant Activities of Polysaccharides from Flowers of *Dendrobium devonianum*. *International Journal of Analytical Chemistry*. 2018; 2018: 3013497.
- [18] Liu J, Han Y, Zhu T, Yang Q, Wang H, Zhang H. *Dendrobium nobile* Lindl. polysaccharides reduce cerebral ischemia/reperfusion injury in mice by increasing myeloid cell leukemia 1 via the downregulation of miR-134. *Neuroreport*. 2021; 32: 177–187.
- [19] Vijayaprakash KM, Sridharan N. An experimental spinal cord injury rat model using customized impact device: A cost-effective approach. *Journal of Pharmacology & Pharmacotherapeutics*. 2013; 4: 211–213.
- [20] Zhang SY, Ji SX, Bai XM, Yuan F, Zhang LH, Li J. L-3-n-butylphthalide attenuates cognitive deficits in db/db diabetic mice. *Metabolic Brain Disease*. 2019; 34: 309–318.
- [21] Fan H, Tang HB, Chen Z, Wang HQ, Zhang L, Jiang Y, *et al*. Inhibiting HMGB1-RAGE axis prevents pro-inflammatory macrophages/microglia polarization and affords neuroprotection after spinal cord injury. *Journal of Neuroinflammation*. 2020; 17: 295.
- [22] Li R, Wu J, Lin Z, Nangle MR, Li Y, Cai P, *et al*. Single injection of a novel nerve growth factor coacervate improves structural and functional regeneration after sciatic nerve injury in adult rats. *Experimental Neurology*. 2017; 288: 1–10.
- [23] Basit F, van Oppen LM, Schöckel L, Bossenbroek HM, van Emst-de Vries SE, Hermeling JC, *et al*. Mitochondrial complex I inhibition triggers a mitophagy-dependent ROS increase leading to necroptosis and ferroptosis in melanoma cells. *Cell Death & Disease*. 2017; 8: e2716.
- [24] Jiang L, Hickman JH, Wang SJ, Gu W. Dynamic roles of p53-mediated metabolic activities in ROS-induced stress responses. *Cell Cycle*. 2015; 14: 2881–2885.
- [25] Dixon SJ, Patel DN, Welsch M, Skouta R, Lee ED, Hayano M, *et al*. Pharmacological inhibition of cystine-glutamate exchange induces endoplasmic reticulum stress and ferroptosis. *eLife*. 2014; 3: e02523.
- [26] Ahuja CS, Nori S, Tetreault L, Wilson J, Kwon B, Harrop J, *et al*. Traumatic Spinal Cord Injury-Repair and Regeneration. *Neurosurgery*. 2017; 80: S9–S22.
- [27] Zhou Y, Wu Y, Liu Y, He Z, Zou S, Wang Q, *et al*. The cross-talk between autophagy and endoplasmic reticulum stress in blood-spinal cord barrier disruption after spinal cord injury. *Oncotarget*. 2017; 8: 1688–1702.
- [28] Anderson MA, O'Shea TM, Burda JE, Ao Y, Barlately SL, Bernstein AM, *et al*. Required growth facilitators propel axon regeneration across complete spinal cord injury. *Nature*. 2018; 561: 396–400.
- [29] Liu D, Huang Y, Jia C, Li Y, Liang F, Fu Q. Administration of antagomir-223 inhibits apoptosis, promotes angiogenesis and functional recovery in rats with spinal cord injury. *Cellular and Molecular Neurobiology*. 2015; 35: 483–491.
- [30] Lin WP, Xiong GP, Lin Q, Chen XW, Zhang LQ, Shi JX, *et al*. Heme oxygenase-1 promotes neuron survival through downregulation of neuronal NLRP1 expression after spinal cord injury. *Journal of Neuroinflammation*. 2016; 13: 52.
- [31] Liu S, Sarkar C, Dinizo M, Faden AI, Koh EY, Lipinski MM, *et al*. Disrupted autophagy after spinal cord injury is associated with ER stress and neuronal cell death. *Cell Death & Disease*. 2015; 6: e1582.
- [32] Ufer C, Wang CC, Föhling M, Schiebel H, Thiele BJ, Billett EE, *et al*. Translational regulation of glutathione peroxidase 4 expression through guanine-rich sequence-binding factor 1 is essential for embryonic brain development. *Genes & Development*. 2008; 22: 1838–1850.
- [33] Zheng J, Conrad M. The Metabolic Underpinnings of Ferroptosis. *Cell Metabolism*. 2020; 32: 920–937.
- [34] Agoston DV. How to Translate Time? The Temporal Aspect of Human and Rodent Biology. *Frontiers in Neurology*. 2017; 8: 92.